Title

Altered Expression and Localization of Ion Transporters Contribute to Diarrhea in Mice With Salmonella-Induced Enteritis

Journal

Gastroenterology, 145(6)

ISSN

0016-5085

Authors

Marchelletta, Ronald R
Gareau, Melanie G
McCole, Declan F
et al.

Publication Date

2013-12-01

DOI

10.1053/j.gastro.2013.08.054

Peer reviewed

Published in final edited form as:
Gastroenterology. 2013 December ; 145(6): 1358–1368.e1-4. doi:10.1053/j.gastro.2013.08.054.

Altered Expression and Localization of Ion Transporters Contribute to Diarrhea in Mice With *Salmonella*-Induced Enteritis

RONALD R. MARCHELLETTA[1,*], **MELANIE G. GAREAU**[1,*], **DECLAN F. MCCOLE**[1], **SHARON OKAMOTO**[2], **ELISE ROEL**[1], **RACHEL KLINKENBERG**[1], **DONALD G. GUINEY**[1], **JOSHUA FIERER**[1,2], and **KIM E. BARRETT**[1]

[1]Department of Medicine, School of Medicine, University of California, San Diego, La Jolla, California

[2]Department of Medicine, VA San Diego Medical Center, San Diego, California

Abstract

BACKGROUND & AIMS—*Salmonella enterica* serovar Typhimurium is an enteropathogen that causes self-limiting diarrhea in healthy individuals, but poses a significant health threat to vulnerable populations. Our understanding of the pathogenesis of *Salmonella*-induced diarrhea has been hampered by the lack of a suitable mouse model. After a dose of oral kanamycin, *Salmonella*-infected congenic BALB/c.D2^{NrampG169} mice, which carry a wild-type *Nramp1* gene, develop clear manifestations of diarrhea. We used this model to elucidate the pathophysiology of *Salmonella*-induced diarrhea.

METHODS—BALB /c.D2^{NrampG169} mice were treated with kanamycin and then infected with wild-type or mutant *Salmonella* by oral gavage. Colon tissues were isolated and Ussing chambers, quantitative polymerase chain reaction, immunoblot, and confocal microscopy analyses were used to study function and expression of ion transporters and cell proliferation.

RESULTS—Studies with Ussing chambers demonstrated reduced basal and/or adenosine 3′,5′-cyclic monophosphate–mediated electrogenic ion transport in infected colonic tissues, attributable to changes in chloride or sodium transport, depending on the segment studied. The effects of infection were mediated, at least in part, by effector proteins secreted by the bacterial *Salmonella* pathogenicity island 1– and *Salmonella* pathogenicity island-2–encoded virulence systems. Infected tissue showed reduced expression of the chloride–bicarbonate exchanger down-regulated in adenoma in surface colonic epithelial cells. Cystic fibrosis transmembrane conductance regulator was internalized in colonic crypt epithelial cells without a change in overall expression levels. Confocal analyses, densitometry, and quantitative polymerase chain reaction revealed that expression of epithelial sodium channel β was reduced in distal colons of *Salmonella*-infected mice. The changes in transporter expression, localization, and/or function were accompanied by crypt hyperplasia in *Salmonella*-infected mice.

Reprint requests Address requests for reprints to: Kim E. Barrett, PhD, Department of Medicine, School of Medicine, University of California, M/C 0003, 9500 Gilman Drive, San Diego, La Jolla, California 92093. kbarrett@ucsd.edu; fax: (858) 534 4304.
*Authors share co-first authorship.
Declan F. McCole's current affiliation is Division of Biomedical Sciences, University of California, Riverside, Riverside, CA.

Conflicts of interest
The authors disclose no conflicts.

Supplementary Material
Note: To access the supplementary material accompanying this article, visit the online version of *Gastroenterology* at www.gastrojournal.org, and at http://dx.doi.org/10.1053/j.gastro.2013.08.054.

CONCLUSIONS—*Salmonella* infection induces diarrhea by altering expression and/or function of transporters that mediate water absorption in the colon, likely reflecting the fact that epithelial cells have less time to differentiate into surface cells when proliferation rates are increased by infection.

Keywords

Salmonella; ENaC; Colon; DRA

Infection with *Salmonella enterica* serovar Typhimurium (henceforth *Salmonella*) is a world-wide health problem common to both industrialized and nonindustrialized countries.[1-3] *Salmonella*-induced diarrhea contributes to the spread of this pathogen, secondary to contamination of food and water supplies.[4] However, little is known about how this pathogen induces diarrhea. In vitro studies with infected colonic epithelial cell lines have suggested modulation of ion transport. However, in vitro models cannot fully recapitulate the effects of infection on physiological responses that produce diarrhea in vivo.[5]

Salmonella relies on 2 type-3 protein secretion systems (T3SS) to invade and spread systemically in the host. *Salmonella* pathogenicity island (SPI)-1 encodes a needle-like protein appendage through which soluble effectors are injected into the host-cell cytosol when in close proximity. These effectors facilitate bacterial uptake into host epithelial cells through manipulation of the cytoskeleton and a variety of signal transduction pathways.[6] The second T3SS, SPI-2, is necessary for maintenance of the integrity of the *Salmonella*-containing vacuole that is essential for intracellular growth in macrophages and systemic spread of the bacteria. SPI-2 translocates bacterial effectors through the phagosomal membrane, which then alter cytoskeletal structures, disrupt membrane trafficking, and affect signal transduction.[6]

The study of *Salmonella*-induced diarrhea is hindered by the fact that oral infection of rodents does not cause enteritis or diarrhea, but if mice are pretreated orally with a nonabsorbed aminoglycoside antibiotic, they will develop colitis.[7] However, many common inbred mouse strains carry a mutant Nramp1 (*Scl11a1*) allele, and after oral infection these mutant mice typically die from systemic salmonellosis without manifesting diarrheal symptoms.[8] The role of Nramp1 is to efflux divalent ions from the phagolysosomes,[9] thereby controlling infection by reducing essential Fe^{2+} and Mn^{2+} required for *Salmonella* growth in the phagolysosome or *Salmonella*-containing vacuole.[10] Without functional Nramp1, mice cannot limit *Salmonella* propagation within macrophages and organisms spread systemically, quickly overwhelming the host without the manifestation of diarrhea.[6] Therefore, we developed a mouse model that exploits congenic BALB/c mice expressing the wild-type (wt) $Nramp1^{G169}$ allele from DBA/2 mice. BALB/c.$D2^{NrampG169}$ mice develop clear manifestations of diarrhea when orally infected with *Salmonella* Typhimurium strain 14028s after pretreatment with kanamycin (Kana), making this mouse an appropriate model for *Salmonella*-induced diarrhea.[11] Within 3 days post infection, stool water content is significantly increased and, by 7–8 days post infection, mice have severe pan-colitis with marked weight loss, colonic shortening, high stool water content, and diarrhea. A high proportion of mice die by 10 days post infection, although the systemic bacterial counts in the liver and spleen are still at sublethal levels, suggesting that the mechanism of death is related to the severe intestinal disease rather than sepsis.[8] Both the SPI-1 and SPI-2 T3SS are required for full enteric virulence in this BALB/c.D2 model of *Salmonella* enteritis.[8,11] A loss of function SPI-1 mutant, *invA*, causes significantly less diarrhea and fecal water content, as well as an absence of inflammatory changes distal to the cecum. A SPI-2 mutant

(*ssaV*) also causes lower fecal water content and markedly reduced colonic inflammation, despite comparable levels of cecal infection compared with wt *Salmonella*.[11]

Therefore, we sought to determine whether *Salmonella* can alter ion transporter function and expression before development of severe colitis and whether these changes contribute to the etiology of diarrhea by altering water absorption. Because SPI-1 and SPI-2 mutants cause attenuated diarrhea and colitis in this model, we used these isogenic mutant strains as specific controls for the virulence effects of *Salmonella* on epithelial physiology and transporter expression.

Materials and Methods

Mouse Model

Ussing chamber experiments used tissue from male and female BALB/c.D2^{NrampG169} congenic mice,[12] and gene expression studies were done with female mice. Mice were bred in-house under specific pathogen–free conditions and allowed free access to food and water. Mice were administered a single dose of Kana (20 mg) by gastric gavage and infected by gavage 48 hours later (5×10^3 colony-forming units of *Salmonella* Typhimurium 14028s in 0.1 mL of 0.1M $NaHCO_3$). Mice were sacrificed by cervical dislocation at 3 days post infection, and all studies were approved by the San Diego VA Institutional Animal Care and Use Committee.

Bacterial Stocks

We constructed a derivative of *Salmonella* Typhimurium 14028s containing a Kana-resistance cassette inserted in a genetically silent region downstream from the *spv* operon.[13] This strain was used as the wt background strain. SPI-1 (*invA*) and SPI-2 (*ssaV*) mutants of 14028s are Kana-resistant and were as described previously.[11,13]

Ussing Chamber Studies

Segments of proximal (first one third from cecum) or distal (last one third to rectum) colon obtained from uninfected and infected mice were stripped of their muscle layers and mounted in Ussing chambers (window area = 0.6 cm^2) according to protocol.[14,15] Tissues were voltage-clamped to zero potential difference by the application of short-circuit current (I_{sc}), and baseline was established. Tissues were treated with adenosine 3′,5′-cyclic monophosphate (forskolin [FSK], 20 μM]) and Ca^{2+} (carbachol, 300 μM]) agonists and the I_{sc} response measured. Under these conditions, changes in I_{sc} (ΔI_{sc}) in response to agonists are largely reflective of electrogenic chloride secretion and/or sodium absorption. For ion substitution studies, sodium isethionate, $CaSO_4$, and $MgSO_4$ were used in place of Cl^- and choline (choline bicarbonate and choline chloride) was used as a substitute for Na^+. Both buffers were supplemented with 10 mmol glucose.

Real-Time Polymerase Chain Reaction

Full-thickness proximal and distal colons were isolated from Kana-treated controls or *Salmonella* (wt and mutants)-infected mice, homogenized using a tissue lyser, and processed using Trizol (Sigma, St Louis, MO) following manufacturer's instructions. The homogenate was then placed on an RNeasy column (Qiagen, Valencia, CA) and RNA isolated and stored at −80°C. RNA was incubated with Turbo DNA-free (Ambion, Austin, TX) before reverse transcription using a high capacity kit (Applied Biosystems, Carlsbad, CA) according to manufacturer's protocol. Primers (IDT, Coralville, IA) used are listed in Supplementary Table 1. All reactions were performed using the Step-One plus system (Applied Bio-systems) under the following conditions: 95°C, 5 minutes; 40 cycles and 95°C, 3 seconds;

60°C 30 seconds. Target genes were normalized to villin. The resulting Ct values were calculated using single delta Ct as $2^{-(\text{Target–Villin})}$ and expressed in arbitrary units.

Western Blot

Full-thickness colonic tissues were excised, placed in RIPA buffer, and lysed using a mini bead beater (BioSpec Products, Inc, Bartlesville, OK). The resulting lysate was spun down and the supernatant removed. Equivalent amounts of protein for each sample were run on a 4%–15% gradient polyacrylamide gel (mini-protean TGX; Bio-Rad, Hercules, CA). After semi-dry transfer, the blot was blocked (5% nonfat milk or 5% bovine serum albumin in phosphate-buffered saline; 1 hour) and incubated with rabbit anti–down-regulated in adenoma (DRA) (kindly provided by Dr Pradeep Dudeja), anti–epithelial sodium channel-β (ENaCβ), anti–cystic fibrosis transmembrane conductance regulator (CFTR), anti–β1ATPase (Genetex, Irvine, CA), anti-*Salmonella* LPS 0-4 [1E6], or anti-NKCC1 (Cell Signaling, MA); and processed according to standard protocols.[16,17] Densitometry was performed using ImageJ software (National Institutes of Health, Bethesda, MD).

Immunofluorescence

Antibodies to DRA (SLC26a3; Sigma; ENaCβ, CFTR, β1ATPase, *Salmonella* lipopolysaccharide 0–4, and NKCC1; Abcam, Cambridge, MA), as well as conjugated secondary antibodies (Alexa Fluor 568 donkey anti-mouse, Alexa Fluor 488 donkey anti-rabbit, and Hoechst 33258; Invitrogen, Carlsbad, CA) were utilized. Colons were removed, rinsed of contents, infused with 4% paraformaldehyde, and "Swiss rolled" (rectum to cecum). The roll was placed in 4% paraformaldehyde, embedded in paraffin, and sectioned (5 μM) onto glass slides. Sections were de-waxed using xylene, hydrated with graded ethanol and heated for antigen retrieval (10mM sodium citrate buffer). The sections were then treated with proteinase K (0.2 μg/mL) Tris-EDTA buffer and blocked (5% bovine serum albumin/2% donkey serum in phosphate-buffered saline). The sections were further blocked with donkey anti-mouse unconjugated Fab fragment (1:10) before immunostaining with primary antibody. Imaging and line scanning were performed using the Zeiss LSM 510 confocal imaging system. Antibodies to NHE3 were generously provided by Dr Mark Donowitz and NHE3 immunostaining was kindly performed by Dr Nicholas Zachos.

Immunohistochemistry

Sections were prepared, cut, and processed as described for immunofluorescence studies. Ki67 antibody (Abcam) was coupled with ABC detection (Vector, Burlingame, CA) followed by AEC chromagen (Vector), and hematoxylin counterstained for visualization. Crypt length was assessed measuring 20 well-oriented, nonadjacent crypts (Nanozoom Digital Image Viewer, Hamamatsu, Japan).

Statistics

All values are presented as means ± SEM for the number of experiments noted. Student's unpaired *t* test or one-way analysis of variance were used as appropriate followed by post-hoc analysis using Bonferroni (quantitative polymerase chain reaction [qPCR]) or Newman-Keuls tests (I_{SC} and ΔI_{SC}). Values of $P < .05$ were considered significant. All analyses were done using GraphPad Prism 4 (La Jolla, CA).

Results

Electrogenic Ion Transport Was Suppressed by Salmonella Infection

Proximal colon was isolated from untreated (Con), Kana-treated, *Salmonella* (wt)-infected, or *Salmonella* mutant–infected (*invA* or *ssaV*) mice and mounted in Ussing chambers.

Baseline resistance (data not shown) showed no difference between treatment groups and histology indicated no significant ulcerations (Supplementary Figure 1). In contrast, baseline I_{sc} (Figure 1) showed a significant decrease between Kana and wt-*Salmonella*–infected groups. Tissue from wt-infected animals had reduced ion transport responses to the adenylate cyclase agonist FSK compared with tissues from control or Kana-treated mice. Neither mutant *Salmonella* decreased sensitivity to FSK (Figure 1*B*). In contrast, transport responses of proximal colon from wt-infected mice to the muscarinic agonist carbachol were not suppressed compared with uninfected control tissues (Figure 1*C*). In the distal colon, baseline transport was also reduced after wt-*Salmonella* infection when compared with Kana-treated, although not significantly (Figure 1*D*), and FSK-mediated ΔI_{sc} responses were significantly reduced (Figure 1*B*). Carbachol-mediated responses were not significantly different between Kana-treated and wt-infected tissues (Figure 1*E*).

Suppression of Electroneutral Transporter Expression in Salmonella-Infected Proximal Colon

Confocal microscopy was used to assess whether infection with *Salmonella* alters localization of the major electroneutral anion transporter, DRA. Confocal microscopy showed that DRA (*green*) remained sharply colocalized with the epithelial intermediate cytoskeletal filament, villin (*purple*) at the apical membrane of proximal colonic surface epithelial cells in uninfected Kana-treated mice (Figure 2*A*). Line scans across the apical membrane of the surface epithelium (*arrows*) showed a decrease in DRA/villin coincident peaks in wt-infected mice corresponding to the reduction in pixel intensity of DRA when compared with Kana-treated and mutant-infected mice. Corresponding findings were obtained when full-thickness proximal colon isolated from Kana-treated and wt-infected mice was analyzed by Western blot (Figure 2*B*). Densitometry showed a significant ($n = 6$; $P < .05$) decrease in DRA in the wt-infected compared with Kana-treated mice. We next assessed whether infection alters messenger RNA (mRNA) levels for the major electroneutral absorptive ion transporters (NHE3 and DRA). qPCR revealed no changes in NHE3 mRNA due to *Salmonella* infection (Supplementary Figure 2), and DRA mRNA was significantly reduced in wt infection compared with Kana-treated tissues or those from mice infected with *invA* or *ssaV* mutants (Figure 2*C*). NHE3 expression in epithelial cells was also not altered by *Salmonella* infection, as determined by microscopy (Supplementary Figure 2). These observations indicate *Salmonella* can reduce the capacity for chloride absorption in the proximal colon and that functional SPI-1 and SPI-2 are necessary for the full suppression of DRA expression.

Altered Trafficking of the Electrogenic Transporter, CFTR, in the Proximal Colon

In Ussing chamber studies, FSK-stimulated electrogenic ion transport (most likely chloride secretion) was diminished by *Salmonella* infection. Using confocal microscopy, CFTR (*green*) was confirmed by line scan to be colocalized with villin (*purple*) to the apical membrane of crypt epithelial cells (*red line, white box*) in control Kana-treated mice (Figure 3*A*). In contrast, CFTR appeared to redistribute to the cytosol in wt-infected mice, as evidenced by the reduction of *green peaks* in the intensity profile. Conversely, the apical localization of CFTR was largely maintained after infection with *ssaV* and *invA* mutants (Figure 3*A*), although there might be partial mislocalization of CFTR in *ssaV* mutant–infected animals. In addition, to eliminate the possibility of modulation of expression or an enhancement of degradation, densitometry (Figure 3*B*) and qPCR (Figure 3*C*) were performed. We observed no difference in CFTR mRNA or protein levels in wt-infected mice vs Kana-treated controls. The reduction of basal and FSK-stimulated I_{sc} seen in wt-infected mice might result from altered CFTR trafficking rather than a reduction in overall expression or degradation.

Reduced ENaC Apical Localization in Wild-Type Salmonella Challenged Distal Colon

The distal colon is an important site for salvage fluid absorption, driven by the Na^+ channel, ENaC. Confocal microscopy of the distal colon from Kana-treated mice showed that ENaCβ (*green*) was localized to a distinct population of surface cells (Figure 4, *arrow*). Staining for ENaCβ was greatly diminished in tissues from wt-infected mice, but not in tissues from mice infected with either the *invA* or *ssaV* mutant (Figure 4). Western blot and densitometry show a significant decrease in ENaCβ, supporting the confocal microscopy. Overall, these findings are consistent with the observed reduction in ion transport in the distal colon from wt-infected mice, which is likely reflective, in part, of reduced electrogenic Na^+ absorption.

ENaC subunits were assessed by qPCR in specimens from mice infected with either wt *Salmonella* or the *invA* and *ssaV* mutants and compared with the Kana-treated control. Wild-type *Salmonella*, but not the *InvA* or *ssaV* mutant, reduced mRNA for ENaCβ (Figure 4*C*). In contrast, mRNA for ENaCα and ENaCγ was not significantly affected by infection with any of the *Salmonella* strains when compared with Kana (Figure 4*C*).

Salmonella-Infected Colons Demonstrate Reduced Electrogenic Cl^- and Na^+ Transport

Ion substitution buffers were employed to establish whether the functional electrogenic ion transport changes we observed in Ussing chambers could be attributed to the altered expression and/or localization of specific ion transporters after *Salmonella* infection. Removal of Cl^- significantly decreased baseline I_{sc} in both kana-treated and wt-infected tissues from the proximal colon (Figure 5*A*). However, removal of Cl^- significantly decreased the ΔI_{sc} response to FSK in the Kana control only, but not in wt-infected tissues (Figure 5*B*). We interpret these data as consistent with the model that the reduced response to FSK in the infected proximal colon can be accounted for, in large part, by the redistribution of CFTR described earlier, because it could not be significantly reduced further by chloride removal. In the distal colon, removal of Na^+ reduced baseline I_{sc} in both Kana-treated and wt-infected tissues, but the effect was more pronounced in uninfected controls (Figure 5*C*). In contrast, the FSK response, whether at control levels in Kana tissues or at reduced levels in tissues from wt-infected mice, was unaffected by removal of Na^+ (Figure 5*D*). We interpret these data to suggest that the reduction in baseline ion transport in infected distal colon is attributable in part to a reduction in ENaC-mediated sodium transport, because Na^+ removal was less effective in reducing I_{sc} values in wt-infected tissues vs Kana controls. By extension, responses to FSK in these tissues do not appear to reflect electrogenic sodium absorption under either condition.

Salmonella-Infected Proximal Colon Demonstrates Aberrant Basolateral Transport

The ion transporter responsible for the cellular loading of Cl^-, NKCC1 (*green*), appeared to be enriched in crypt epithelial cells in Kana-treated proximal colon (Supplementary Figure 3*A*) with exclusive basolateral localization when referenced to villin (*red:* apical). The NKCC1-enriched cell population appears to expand in wt-infected colon (Supplementary Figure 3*A*). This increase in NKCC1-enriched cells was not observed in SPI-1 or SPI-2 mutant–infected mice (Supplementary Figure 3*A*). In addition, Western blot and qPCR did not show a significant increase in NKCC1 protein (Supplementary Figure 3*B*) or gene expression (Supplementary Figure 3*C*) in wt-infected mice compared with Kana-treated controls (when normalized for cellular proteins), probably because the amount of NKCC1 per cell was unchanged. In summary, this suggests that the increase in NKCC1 seen in tissue sections is not due to changes in gene or protein expression but rather to an increase in NKCC1-enriched crypt cells (described in findings of epithelial crypt hyperplasia).

Mice Infected With Wild-Type Salmonella Have Reduced Expression of β1ATPase

Confocal microscopy reveals that mice infected with wt *Salmonella* show a reduced basolateral localization β1ATPase (*green*) as referenced to the apical localization of villin (*purple*) and intracellular nuclei (*blue*; Supplementary Figure 4). In addition, in wt-infected tissues, β1ATPase and villin appeared inappropriately co-localized in surface cells, perhaps suggesting that basolateral and apical membrane domains are no longer fully segregated. Densitometry also supported confocal observations of reduced β1ATPase protein levels in wt-infected versus Kana-treated mice.

Salmonella Causes Epithelial Crypt Hyperplasia

In the proximal colon, an increased number of epithelial cells stained positively for the proliferation marker, Ki67, in wt *Salmonella*–infected tissues compared with Kana-treated controls (Figure 6*A*). This increase was not observed in either *invA* or *ssaV* mutant–infected tissues. An increase in colonic crypt depth was also observed in *Salmonella*-infected tissues compared with Kana controls (Figure 6*B* and *C*). Together, this suggests that crypt hyperplasia is driven by cell proliferation in response to wt-*Salmonella* infection.

Functional Effects of Salmonella Infection Are Not Restricted to Infected Cells

Confocal microscopy was utilized to determine whether the effects of *Salmonella* infection were restricted to infected epithelial cells or whether they were generalized. Wild-type *Salmonella* were clearly localized within a minor population of surface epithelial cells, but none were detected in the crypts (Figure 7*A* and *D*). In contrast, fewer *ssaV* mutant bacteria were detected in the surface epithelium and none were seen in crypts (Figure 7*B* and *E*), and *invA* mutants were exclusively localized to the intestinal lumen (Figure 7*C* and *F*). Because wt *Salmonella* infected only a small percentage of epithelial cells, ion transport modulation by wt *Salmonella* infection is not restricted to epithelial cells that have been directly invaded by *Salmonella*, but rather represents a more generalized response of host colonocytes to this infection.

Discussion

Functional analysis of electrogenic ion transport and transporter expression and localization studies suggest that *Salmonella* modulates colonic ion transport and this requires the bacterial T3SS systems encoded by SPI-1 and SPI-2 virulence loci. Ussing chamber studies of wt *Salmonella*–infected mice showed aberrations in ion transport function when compared with uninfected or mutant-infected mice in both proximal and distal colon. Neither segment showed barrier dysfunction or evidence of ulcerations (Supplementary Figure 1). *Salmonella*-induced modulation of ion transport could induce diarrhea in the affected host, through either decreased absorption or increased secretion of water and electrolytes.[18] In fact, enteropathogens have been reported to modulate ion transporters in epithelial cell lines via effectors injected through their T3SS.[17,19,20] Similarly, *Citrobacter rodentium* infection of mouse colons decreased expression of DRA.[14] Loss-of-function mutations in DRA cause congenital chloride-mediated diarrhea.[21] In addition, the *Salmonella* SPI-1 Sop E effector family has homology with the EPEC T3SS effector Map, which has been implicated in indirect regulation of DRA, CFTR, and NHE3.[22-25] In addition, the major transporter responsible for the uptake of Na^+ in the distal colon, ENaC, is down-regulated by lipopolysaccharide via nuclear factor-κB– mediated inhibition of SGK1.[26] Finally, in the lung, *Pseudomonas aeruginosa* decreases mRNA for ENaC subunits.[27] Comparisons of proximal and distal colon from mice treated with Kana only or subsequently infected with either wt or mutant *Salmonella* revealed that there was profound modulation of ion transport that likely underlies, at least in part, the diarrhea associated with wt *Salmonella* infection.[28,29] In particular, the reduced ability of sodium removal to

abrogate baseline I_{sc} in wt-infected vs Kana-treated distal colon argues that tonic salvage fluid absorption in infected tissues is likely reduced secondary to the loss of ENaC expression.

Confocal analysis also revealed a reduction in DRA (but not NHE3) apical localization in surface cells of the proximal colon from wt-infected mice compared with Kana-treated or mutant-infected mice. Both DRA protein and mRNA are reduced in wt-infected mice. However, because this transporter is electroneutral, the decrease in DRA expression does not explain the defect in electrogenic transport responses observed in colonic epithelium from wt-infected mice. Nevertheless, the decrease in DRA in wt-infected mice could increase luminal Cl^- concentrations, retaining water in the luminal space and contributing to diarrhea.

Expression of CFTR appeared to be mislocalized in crypt cells in the proximal colon of wt-infected mice compared with controls. Because CFTR mediates electrogenic Cl^- transport, this aberrant localization might underpin the reduction in basal I_{sc}, because CFTR likely contributes to baseline secretion.[30] In addition, CFTR internalization could explain the reduction in FSK-stimulated ΔI_{sc} in wt-infected mice. The fact that qPCR and densitometry revealed no change in overall CFTR expression supports that aberrant CFTR trafficking, and not lower expression, explains the loss of function. Reduced I_{sc} responses to FSK in wt-infected tissues are also likely attributable to the loss of apical CFTR because they were no longer sensitive to chloride removal. Nevertheless, redistribution of CFTR and a subsequent decrease in Cl^- secretion cannot directly account for *Salmonella*-induced diarrhea, although a relative failure of crypt secretory function might ultimately be expected to compromise crypt sterility and barrier function.

Wild-type *Salmonella* infection was associated with hyperplasia of crypt cells, similar to that observed in the setting of *C rodentium* infection in mice.[31] The proliferative response may represent an attempt by the host to shed bacterially infected cells at the expense of cellular differentiation across the length of the crypt. Although NKCC1 was highly enriched in crypt cells of the proximal colon in controls, in wt-infected mice, NKCC1-positive cells extended further up the crypt when compared with the Kana-treated and mutant *Salmonella* controls. However, neither protein nor mRNA analyses revealed a change in normalized NKCC1 expression between Kana-treated and wt-infected mice, suggesting that the confocal findings reflected an increased number of NKCC1-positive cells rather than increased protein expression per cell. The increased epithelial proliferation in wt-infected mice further supports our model of an immature epithelium that contributes to the diarrhea. In addition, NKCC1 was diffusely localized in infected tissues compared with the sharp basolateral localization in controls. In fact, a reduction in basolateral NKCC1, as well as β1ATPase, could contribute to the suppression of basal electrogenic transport by wt *Salmonella* in the proximal colon.

Salmonella infection resulted in bacterial colonization throughout the colon by day 3 post infection, but the distal colon had 10-fold fewer bacteria/gram of tissue than did the proximal colon (data not shown).[11] By confocal microscopy, the *ssaV* mutant appeared to be present in epithelial tissue to a lesser extent than the wt, and the *invA* mutant was not observed to translocate from the lumen. These findings agree with earlier observations in the *Salmonella*-infected rat colon demonstrating distal effects of *Salmonella* on transport function.[32]

Overall, our results support a model in which *Salmonella* infection of the colon produces early inflammatory changes that drive compensatory epithelial proliferation and thereby alter the physiology of ion transporters via expression and functional localization. Events

occurring solely in epithelial cells directly infected by *Salmonella* are unlikely to account for all of the early physiologic manifestations of diarrhea; rather, our data suggest the importance of diffusible factors that link *Salmonella* infection to overall epithelial proliferation and ion transport physiology. *Salmonella* has been shown to induce mediators of intestinal epithelial cell proliferation through specific inflammatory pathways that include production of interleukin-17/interleukin-22, interleukin-18, and granulocyte-macrophage colony-stimulating factor.[33-35] In addition, *Salmonella* infection activates the *β*-catenin/Wnt pathway.[36] *Salmonella*-induced intestinal inflammation can promote the colonization phase of enteric infection through the modulation of specific conditions, including antimicrobial peptides and metabolic factors, favoring its growth over the resident microbiota.[35] Our results indicate that *Salmonella*-induced inflammation likely also induces diarrhea through changes in epithelial cell proliferation and the expression and function of ion transporters that lead to decreased absorptive function in the colon. The combined effect of these virulence mechanisms on host inflammatory responses ensures both intestinal colonization and increased transmission of this enteric pathogen.

In conclusion, *Salmonella* infection modulates colonic ion transport at an early stage in experimental colitis, in part due to increased epithelial cell proliferation influencing absorptive epithelial function. Although the physiological effects of infection are not limited to absorptive transport, the suppression of absorption would be expected to cause an accumulation of luminal fluid as an important contributor to *Salmonella*-induced diarrhea that precedes frank dysentery in this model. Many patients with *Salmonella* enteritis present mainly with diarrhea. Therefore, strategies to restore absorptive transport would be expected to be beneficial in *Salmonella* gastroenteritis.

Supplementary Material

Refer to Web version on PubMed Central for supplementary material.

Acknowledgments

Funding

Supported by grants 1 R01 AI077661-01A1 (DGG, JF, KEB), UC San Diego Digestive Diseases Research and Development Center, NIH DK080506 (KEB); NIH T32 DK07202 (RRM), and a VA Merit Review Grant (JF).

References

1. Shaheen NJ, Hansen RA, Morgan DR, et al. The burden of gastrointestinal and liver diseases, 2006. Am J Gastroenterol. 2006; 101:2128–2138. [PubMed: 16848807]
2. Everhart, JE., editor. US Department of Health and Human Services, Public Health Service, National Institutes of Health, National Institute of Diabetes and Digestive and Kidney Diseases. Washington, DC: US Government Printing Office; 2008. The Burden of Digestive Diseases in the United States. NIH Publication No. 09–6443
3. Kosek M, Bern C, Guerrant RL. The global burden of diarrhoeal disease, as estimated from studies published between 1992 and 2000. Bull World Health Organ. 2003; 81:197–204. [PubMed: 12764516]
4. Lloyd-Evans N, Pickering HA, Goh SG, et al. Food and water hygiene and diarrhoea in young Gambian children: a limited case control study. Trans R Soc Trop Med Hyg. 1984; 78:209–211. [PubMed: 6380015]
5. Bertelsen LS, Paesold G, Marcus SL, et al. Modulation of chloride secretory responses and barrier function of intestinal epithelial cells by the *Salmonella* effector protein SigD. Am J Physiol Cell Physiol. 2004; 287:C939–C948. [PubMed: 15175224]

6. Haraga A, Ohlson MB, Miller SI. *Salmonella*e interplay with host cells. Nat Rev Microbiol. 2008; 6:53–66. [PubMed: 18026123]
7. Bohnhoff M, Drake BL, Miller CP. Effect of streptomycin on susceptibility of intestinal tract to experimental *Salmonella* infection. Proc Soc Exp Biol Med. 1954; 86:132–137. [PubMed: 13177610]
8. Woo H, Okamoto S, Guiney D, Gunn JS, Fierer J. A model of *Salmonella* colitis with features of diarrhea in SLC11A1 wild-type mice. PLoS One. 2008; 3:e1603. [PubMed: 18270590]
9. Jabado N, Jankowski A, Dougaparsad S, et al. Natural resistance to intracellular infections: natural resistance-associated macrophage protein 1 (Nramp1) functions as a pH-dependent manganese transporter at the phagosomal membrane. J Exp Med. 2000; 192:1237–1248. [PubMed: 11067873]
10. Lam-Yuk-Tseung S, Picard V, Gros P. Identification of a tyrosine-based motif (YGSI) in the amino terminus of Nramp1 (Slc11a1) that is important for lysosomal targeting. J Biol Chem. 2006; 281:31677–31688. [PubMed: 16905747]
11. Fierer J, Okamoto S, Banerjee A, Guiney DG. Diarrhea and colitis in mice require the *Salmonella* pathogenicity island 2-encoded secretion function but not SifA or Spv effectors. Infect Immun. 2012; 80:3360–3370. [PubMed: 22778101]
12. Potter M, O'Brien AD, Skamene E, et al. A BALB/c congenic strain of mice that carries a genetic locus (Ityr) controlling resistance to intracellular parasites. Infect Immun. 1983; 40:1234–1235. [PubMed: 6343242]
13. Lesnick ML, Reiner NE, Fierer J, et al. The *Salmonella* spvB virulence gene encodes an enzyme that ADP-ribosylates actin and destabilizes the cytoskeleton of eukaryotic cells. Mol Microbiol. 2001; 39:1464–1470. [PubMed: 11260464]
14. Spehlmann ME, Dann SM, Hruz P, et al. CXCR2-dependent mucosal neutrophil influx protects against colitis-associated diarrhea caused by an attaching/effacing lesion-forming bacterial pathogen. J Immunol. 2009; 183:3332–3343. [PubMed: 19675161]
15. McCole DF, Rogler G, Varki N, et al. Epidermal growth factor partially restores colonic ion transport responses in mouse models of chronic colitis. Gastroenterology. 2005; 129:591–608. [PubMed: 16083715]
16. Saksena S, Singla A, Goyal S, et al. Mechanisms of transcriptional modulation of the human anion exchanger SLC26A3 gene expression by IFN-{gamma}. Am J Physiol Gastrointest Liver Physiol. 2010; 298:G159–G166. [PubMed: 19940027]
17. Gill RK, Borthakur A, Hodges K, et al. Mechanism underlying inhibition of intestinal apical Cl/OH exchange following infection with enteropathogenic E. coli. J Clin Invest. 2007; 117:428–437. [PubMed: 17256057]
18. Barrett, KE. Gastrointestinal Physiology. Vol. xiv. New York: Lange Medical Books/McGraw-Hill, Medical Publishing Division; 2006. p. 295
19. Hecht G, Hodges K, Gill RK, et al. Differential regulation of Na+/H+ exchange isoform activities by enteropathogenic E. coli in human intestinal epithelial cells. Am J Physiol Gastrointest Liver Physiol. 2004; 287:G370–G378. [PubMed: 15075254]
20. Borthakur A, Gill RK, Hodges K, et al. Enteropathogenic Escherichia coli inhibits butyrate uptake in Caco-2 cells by altering the apical membrane MCT1 level. Am J Physiol Gastrointest Liver Physiol. 2006; 290:G30–G35. [PubMed: 16150873]
21. Dorwart MR, Shcheynikov N, Baker JM, et al. Congenital chloride-losing diarrhea causing mutations in the STAS domain result in misfolding and mistrafficking of SLC26A3. J Biol Chem. 2008; 283:8711–8722. [PubMed: 18216024]
22. Bulgin R, Raymond B, Garnett JA, et al. Bacterial guanine nucleotide exchange factors SopE-like and WxxxE effectors. Infect Immun. 2010; 78:1417–1425. [PubMed: 20123714]
23. Simpson N, Shaw R, Crepin VF, et al. The enteropathogenic Escherichia coli type III secretion system effector Map binds EBP50/NHERF1: implication for cell signalling and diarrhoea. Mol Microbiol. 2006; 60:349–363. [PubMed: 16573685]
24. Borenshtein D, Fry RC, Groff EB, et al. Diarrhea as a cause of mortality in a mouse model of infectious colitis. Genome Biol. 2008; 9:R122. [PubMed: 18680595]
25. Lamprecht G, Heil A, Baisch S, et al. The down regulated in adenoma (dra) gene product binds to the second PDZ domain of the NHE3 kinase A regulatory protein (E3KARP), potentially linking

intestinal Cl-/HCO3- exchange to Na+/H+ exchange. Biochemistry. 2002; 41:12336–12342. [PubMed: 12369822]

26. de Seigneux S, Leroy V, Ghzili H, et al. NF-kappaB inhibits sodium transport via down-regulation of SGK1 in renal collecting duct principal cells. J Biol Chem. 2008; 283:25671–25681. [PubMed: 18586672]
27. Dagenais A, Gosselin D, Guilbault C, et al. Modulation of epithelial sodium channel (ENaC) expression in mouse lung infected with Pseudomonas aeruginosa. Respir Res. 2005; 6:2. [PubMed: 15636635]
28. Talbot C, Lytle C. Segregation of Na/H exchanger-3 and Cl/HCO3 exchanger SLC26A3 (DRA) in rodent cecum and colon. Am J Physiol Gastrointest Liver Physiol. 2010; 299:G358–G367. [PubMed: 20466943]
29. Alper SL, Stewart AK, Vandorpe DH, et al. Native and recombinant Slc26a3 (downregulated in adenoma, Dra) do not exhibit properties of 2Cl-/1HCO3- exchange. Am J Physiol Cell Physiol. 2011; 300:C276–C286. [PubMed: 21068358]
30. Clarke LL, Harline MC. Dual role of CFTR in cAMP-stimulated HCO3-secretion across murine duodenum. Am J Physiol. 1998; 274:G718–G726. [PubMed: 9575854]
31. Wine E, Shen-Tu G, Gareau MG, et al. Osteopontin mediates Citrobacter rodentium-induced colonic epithelial cell hyperplasia and attaching-effacing lesions. Am J Pathol. 2010; 177:1320–1332. [PubMed: 20651246]
32. Powell DW, Plotkin GR, Maenza RM, et al. Experimental diarrhea. I. Intestinal water and electrolyte transport in rat *Salmonella* enterocolitis. Gastroenterology. 1971; 60:1053–1064. [PubMed: 5556910]
33. Huber S, Gagliani N, Zenewicz LA, et al. IL-22BP is regulated by the inflammasome and modulates tumorigenesis in the intestine. Nature. 2012; 491:259–263. [PubMed: 23075849]
34. Egea L, McAllister CS, Lakhdari O, et al. GM-CSF produced by non-hematopoietic cells is required for early epithelial cell proliferation and repair of injured colonic mucosa. J Immunol. 2013; 190:1702–1713. [PubMed: 23325885]
35. Broz P, Ohlson MB, Monack DM. Innate immune response to *Salmonella* typhimurium, a model enteric pathogen. Gut Microbes. 2012; 3:62–70. [PubMed: 22198618]
36. Martinez Rodriguez NR, Eloi MD, Huynh A, et al. Expansion of Paneth cell population in response to enteric *Salmonella* enterica serovar Typhimurium infection. Infect Immun. 2012; 80:266–275. [PubMed: 22006567]

Abbreviation used in this paper

CFTR	cystic fibrosis transmembrane conductance regulator
DRA	down-regulated in adenoma
ENaC	epithelial sodium channel
FSK	forskolin
Kana	kanamycin
mRNA	messenger RNA
qPCR	quantitative polymerase chain reaction
SPI	*Salmonella* pathogenicity island
T3SS	type-3 protein secretion system
wt	wild-type

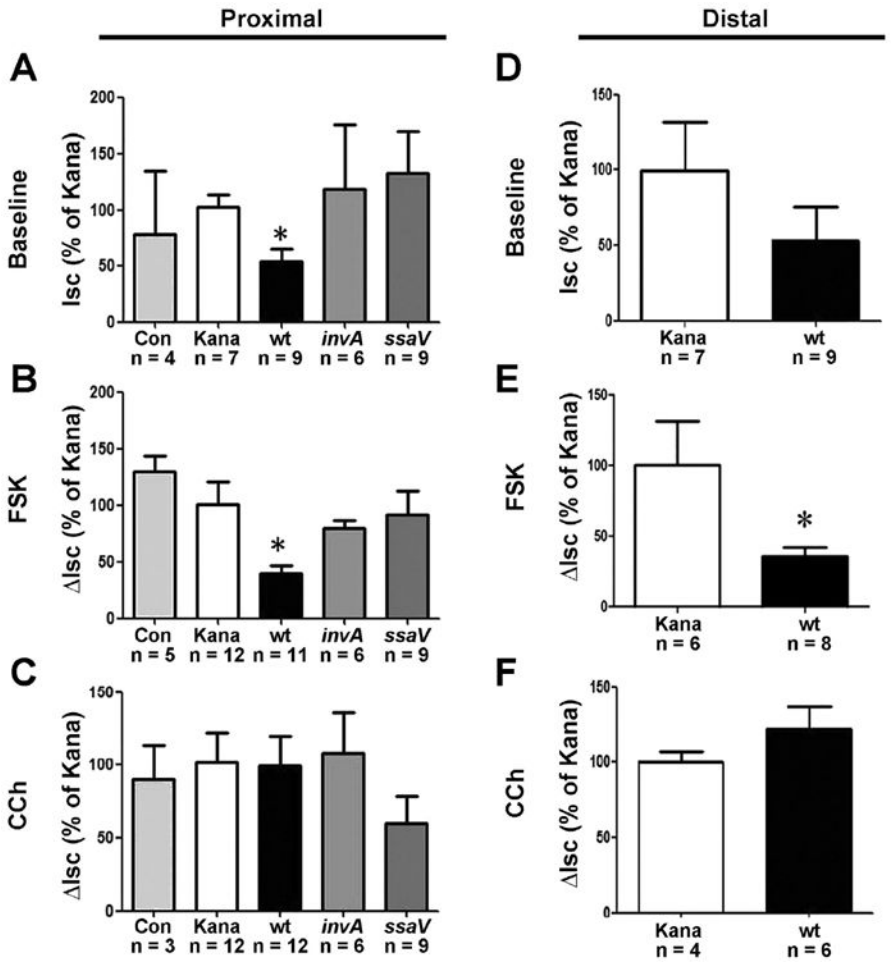

Figure 1.

wt *Salmonella* inhibits adenosine 3′,5′-cyclic monophosphate–dependent ion transport in proximal and distal colon. In the proximal colon, baseline I_{sc} (*A*), and I_{sc} responses to FSK (*B*) and carbachol (CCh [C]) were determined in control (Con), Kana-treated or *Salmonella*-infected (wt, *invA, ssaV* mutants) mice (**P* < .05; analysis of variance [ANOVA]). Similarly, in the distal colon, baseline I_{sc} (*D*) and I_{sc} responses to FSK (*E*) and CCh (*F*) stimulation were compared for wt and Kana-treated mice (**P* < .05; Student's *t* test, with data was normalized to the Kana control).

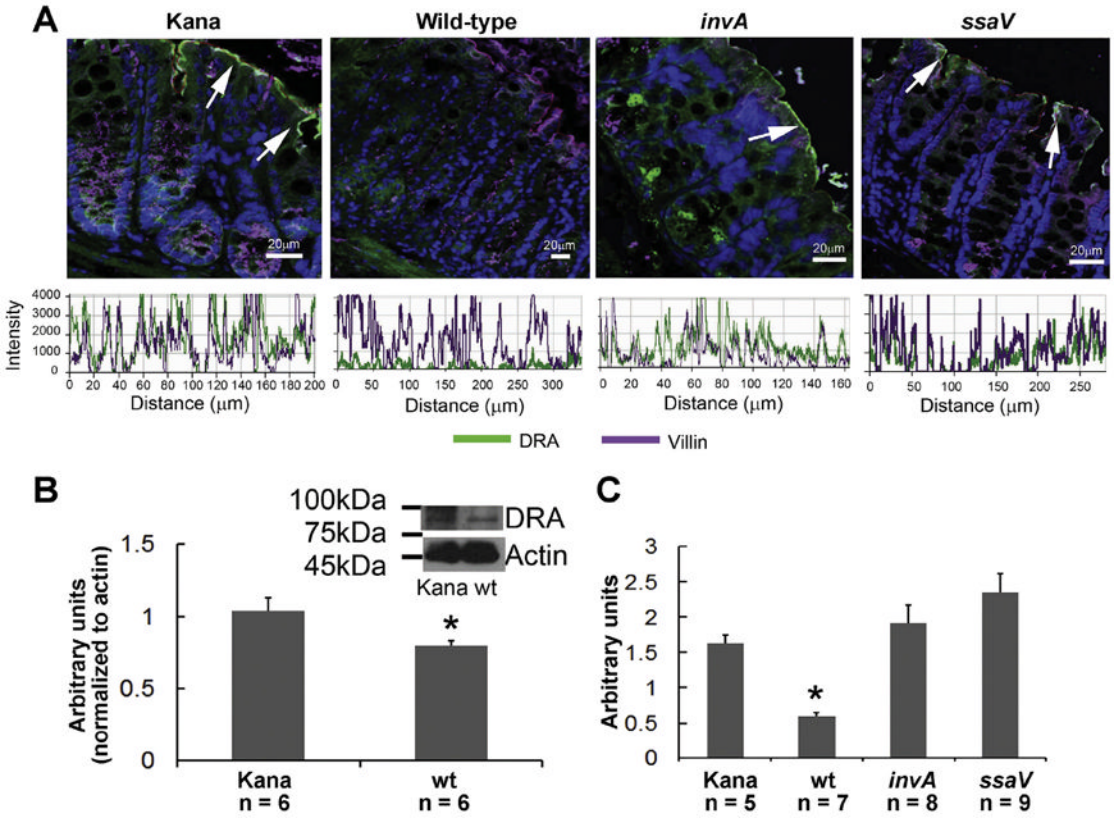

Figure 2.

Apical localization of DRA in surface epithelial cells of the proximal colon is reduced by wt *Salmonella* infection. Confocal imaging of DRA (*green*) and villin (*purple*) in proximal colon from control (Con), kanamycin-treated (Kana) or *Salmonella*-infected (wt, *invA*, or *ssaV* mutants) mice (*A*). Line scans (*red*) quantify DRA colocalization with villin (*white*) at the apical membrane of surface epithelial cells (*arrows*). All images are representative of 6–10 fields from n = 2–3 experiments (scale bar = approximately 20 μm); Hoechst-stained nuclei (*blue*). Western blot (*inset*) and densitometry (*B*) for DRA protein (*$P < .05$; Student's *t* test). mRNA levels (*C*) for DRA (*$P < .05$; analysis of variance).

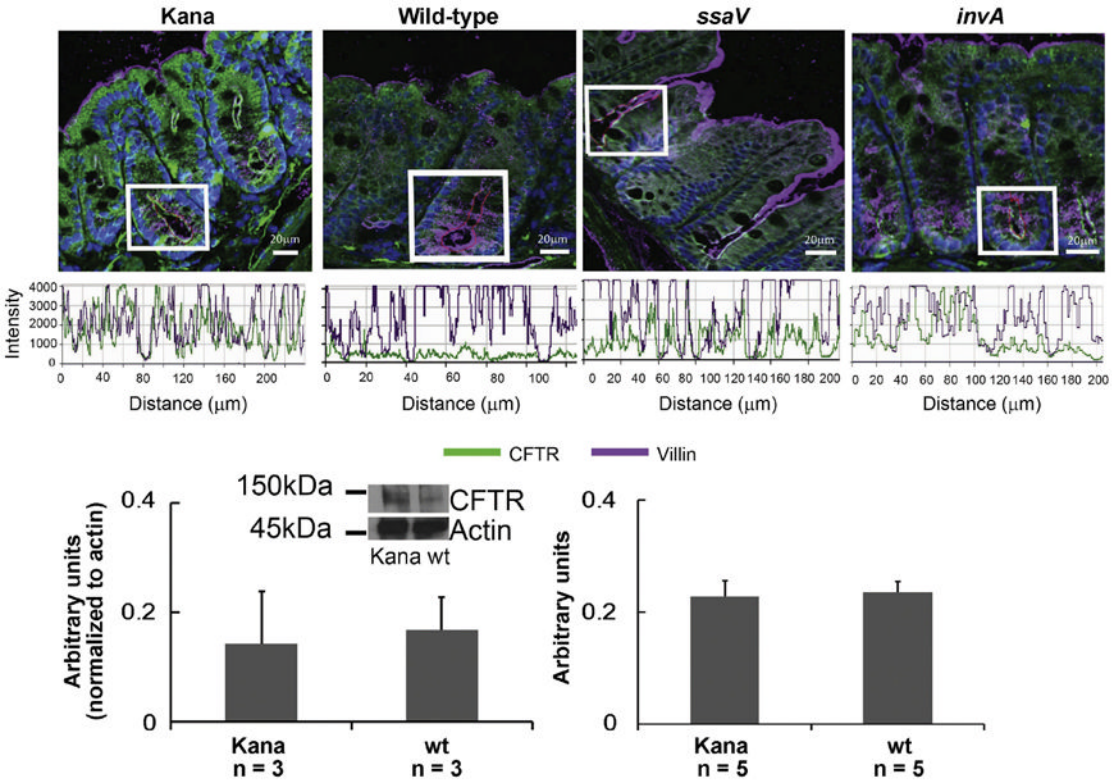

Figure 3.

CFTR is internalized in proximal colon from wt-infected mice. Confocal imaging of CFTR (*green*) and villin (*purple*) in proximal colon from control (Con), Kana-treated or *Salmonella*-infected (wt, *invA*, or *ssaV* mutants) mice (*A*). CFTR colocalization with the apical membrane marker, villin, in crypt epithelial cells (*box*) was determined by line scans in selected crypts (*white box*). All images are representative of 6–10 fields from n = 2–3 experiments (scale bar = approximately 20 μm); Hoechst-stained nuclei (*blue*). Western blot (*inset*) and densitometry (*B*) for CFTR protein and qPCR (*C*) for CFTR mRNA.

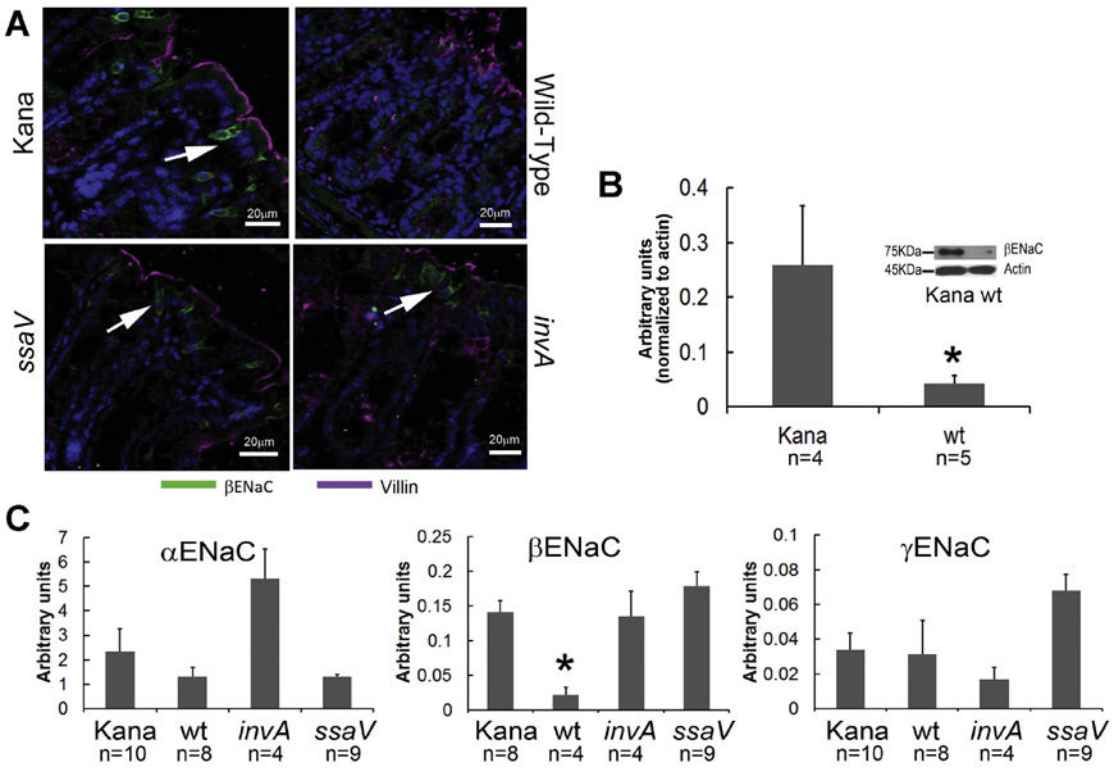

Figure 4.

ENaC*β*-enriched cells are reduced in wt-infected mice. Confocal imaging of ENaC*β* (*green*) and the apical membrane marker, villin (*purple*) in distal colon from control (Con), Kana-treated or *Salmonella*-infected (wt, *invA*, or *ssaV* mutants) mice (*A*). *Arrows* represent epithelial cells enriched in ENaC*β*. All images are representative of 6–10 fields from n = 2–3 experiments; Hoechst-stained nuclei (*blue*). Western blot (*inset*) and densitometry (*B*) for ENaC*β* protein (**P* < .05; Student's *t* test). mRNA levels (*C*) for ENaC*α*, *β*, and *γ* (**P* < .05; analysis of variance).

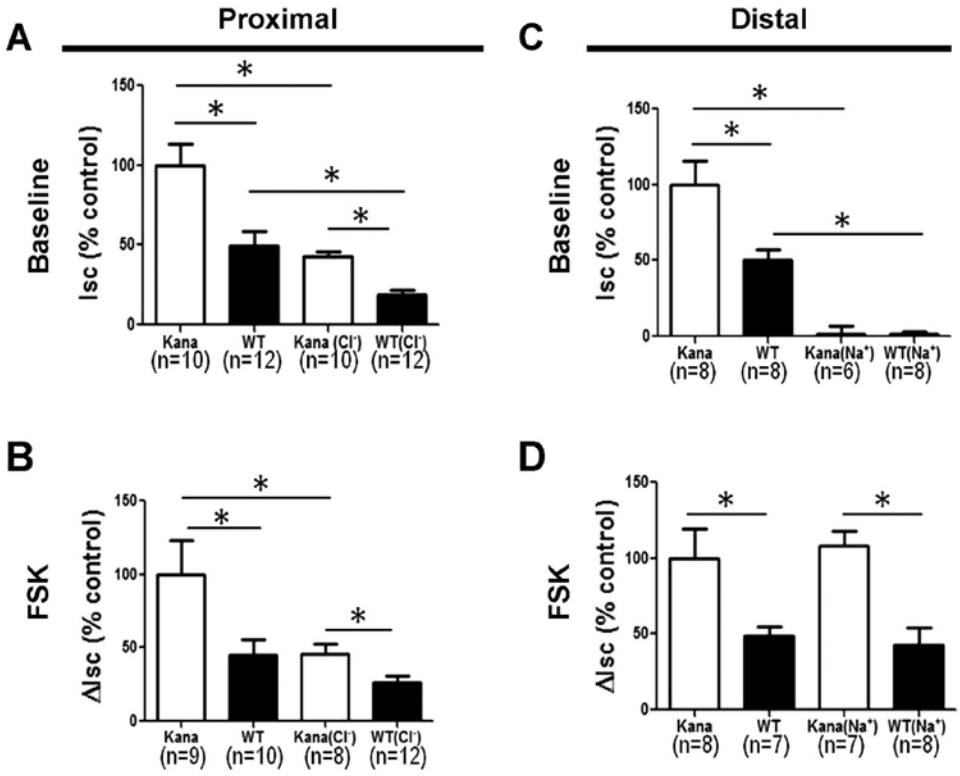

Figure 5.

Ion substitution reveals reduced Cl^- and Na^+ transport in proximal and distal colon, respectively, from mice infected with wt *Salmonella*. Baseline I_{sc} (*A, C*) and FSK-stimulated I_{sc} responses (*B, D*) were measured in Ringer's solution, or in the absence of Cl^- (proximal, Kana [Cl^-] or wt [Cl^-]) or Na^+ (distal, Kana [Na^+] or wt [Na^+]) ions (*$P < .05$; analysis of variance).

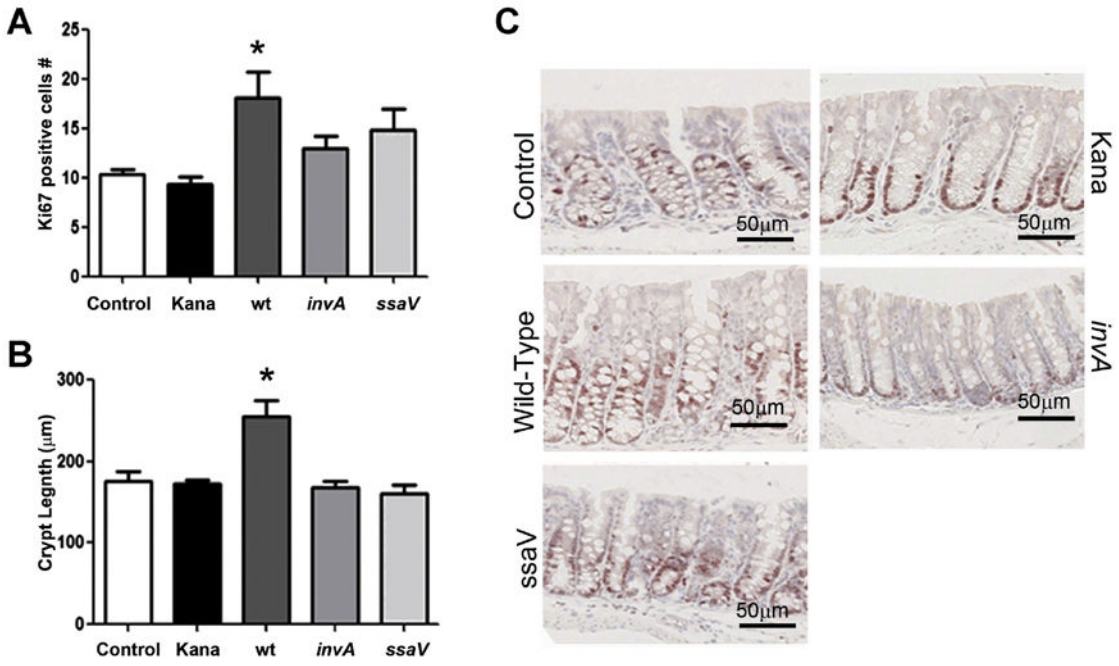

Figure 6.

Epithelial cell proliferation and colonic hyperplasia after *Salmonella* infection. Staining for the proliferation marker Ki67 was performed, followed by quantification of positive cells from control (Con), Kana-treated, or *Salmonella*-infected (wt, *invA*, or *ssaV* mutants) mouse proximal colonic tissue (*A*). Colonic epithelial cell hyperplasia (*B*) was assessed by measuring crypt depth. Representative images (*C*) (*$P < .05$; analysis of variance, n = 3–4 from 2 experiments).

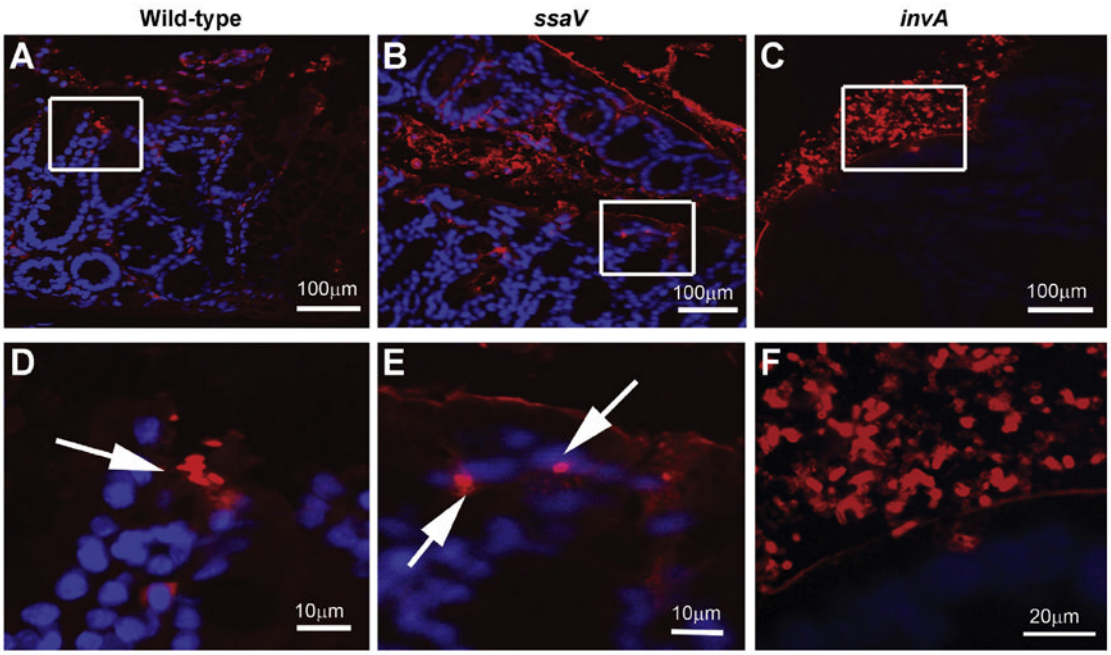

Figure 7.

Translocation of invA and ssaV mutant *Salmonella* is attenuated compared with wt *Salmonella*. Confocal imaging of *Salmonella* (*red*) in proximal colon from infected (wt, *invA*, or *ssaV* mutants) mice (*A–F*). Lower panels (*D–F*) are magnified images of the corresponding *boxed areas*. Bacteria (*white arrows*); Hoechst-stained nuclei (*blue*). All images are representative of 6–10 fields from n = 2–3 experiments.